

*Citation for published version:*

Matamoros-Veloza, A, Hossain, KMZ, Scammell, BE, Ahmed, I, Hall, R & Kapur, N 2020, 'Formulating injectable pastes of porous calcium phosphate glass microspheres for bone regeneration applications', *Journal of the Mechanical Behavior of Biomedical Materials*, vol. 102, 103489. <https://doi.org/10.1016/j.jmbbm.2019.103489>

*DOI:*

[10.1016/j.jmbbm.2019.103489](https://doi.org/10.1016/j.jmbbm.2019.103489)

*Publication date:*

2020

*Document Version*

Peer reviewed version

[Link to publication](#)

*Publisher Rights*

CC BY-NC-ND

**University of Bath**

**Alternative formats**

If you require this document in an alternative format, please contact:  
[openaccess@bath.ac.uk](mailto:openaccess@bath.ac.uk)

**General rights**

Copyright and moral rights for the publications made accessible in the public portal are retained by the authors and/or other copyright owners and it is a condition of accessing publications that users recognise and abide by the legal requirements associated with these rights.

**Take down policy**

If you believe that this document breaches copyright please contact us providing details, and we will remove access to the work immediately and investigate your claim.

## **Formulating injectable pastes of porous calcium phosphate glass microspheres for bone regeneration applications**

Adriana Matamoros-Veloza<sup>1,\*</sup>, Kazi M. Zakir Hossain<sup>2,3</sup>, Brigitte E. Scammell<sup>4</sup>, Ifty Ahmed<sup>2</sup>, Richard Hall<sup>1</sup>, Nikil Kapur<sup>1,\*</sup>

<sup>1</sup>School of Mechanical Engineering, University of Leeds, LS2 9JT, UK

<sup>2</sup>Faculty of Engineering, Advanced Materials Research Group, University of Nottingham, NG7 2RD, UK

<sup>3</sup>Department of Chemistry, University of Bath, Claverton Down, Bath, BA2 7AY, UK

<sup>4</sup>Faculty of Medicine & Health Sciences, Queen's Medical Centre, Nottingham, UK

\*Email: [A.MatamorosVeloza@leeds.ac.uk](mailto:A.MatamorosVeloza@leeds.ac.uk), [n.kapur@leeds.ac.uk](mailto:n.kapur@leeds.ac.uk)

### **Abstract**

Current trends in regenerative medicine treatments for bone repair applications focus on cell-based therapies. These aim to deliver the treatment via a minimally invasive injection to reduce patient trauma and to improve efficacy. This paper describes the injectability of porous calcium phosphate glass microspheres to be used for bone repair based on their formulation, rheology and flow behavior. The use of excipients (xanthan gum, methyl cellulose and carboxyl methyl cellulose) were investigated to improve flow performance. Based on our results, the flow characteristics of the glass microsphere pastes vary according to particle size, surface area, and solid to liquid ratio, as well as the concentration of viscosity modifiers used. The optimal flow characteristics of calcium phosphate glass microsphere pastes was found to contain 40 mg/mL of xanthan gum which increased viscosity whilst providing elastic properties (~ 29000 Pa) at shear rates that mirror the injection process and the

resting period post injection, preventing the glass microspheres from both damage and dispersion. It was established that a base formulation must contain 1g of glass microspheres (60 - 125  $\mu\text{m}$  in size) per 1 mL of cell culture media, or 0.48g of glass microspheres of sizes between 125 and 200  $\mu\text{m}$ . Furthermore, the glass microsphere formulations with xanthan gum were readily injectable via a syringe-needle system (3-20 mL, 18G and 14G needles), and have the potential to be utilized as a cell (or other biologics) delivery vehicle for bone regeneration applications.

**Keywords:** Osteoporosis, bone regeneration, minimal invasive technology, injectable paste, porous microspheres

## 1. Introduction

Osteoporosis is a disease that reduces bone density deteriorating its internal microstructure and increasing the risk of fracture. People over 65 are at higher risk of developing osteoporosis with more than 22 million being affected in the EU.<sup>1</sup> Women are significantly affected by osteoporosis as a consequence of the menopause. In the UK, statistics indicate that 1 in 2 women over 50 experience osteoporotic fractures in comparison to 1 in 5 men.<sup>1,2</sup> The most common and more debilitating fractures occur in hips accounting for 70% in women and 20% in men, with high index of mortality within six months after fracture.<sup>3-5</sup> One of the most frequent drug treatments for osteoporosis patients includes the administration of bisphosphonates which have been reported to be highly effective in reducing the risk of hip fractures (~30-50%). However, patients receiving this drug treatment still suffer subsequent fractures within 3 years.<sup>4, 6-11</sup> Therefore, recent alternative approaches to promote bone healing explore the use of biomaterials and cell-based therapy to improve biocompatibility.<sup>12-</sup>  
<sup>14</sup> Stem cells have already shown their capability in regenerating new bone;<sup>15-17</sup>

however, the fragility of stem cells requires a robust technology to protect them during transplantation and within the timeframe for regeneration of the damaged bone.

Recently, Hossain et al. (2018) developed an innovative approach to manufacture porous glass microspheres produced from calcium phosphates, a key component in bones, which have shown efficacy to incorporate stem cells within their porous structure.<sup>18</sup> One of the key suggested advantages of microspheres over irregular-shaped materials is their potential ability to enhance flow properties, which combined with their microscale size could enable their delivery via minimally invasive injection procedures.<sup>19</sup> In addition, calcium phosphate (CaP) glasses have been widely investigated for hard tissue engineering applications.<sup>20-24</sup> The main benefit of CaP glasses is their degradability and controllable resorption profiles, which can be tailored from days to months by simply altering their composition.<sup>25</sup> Moreover, the porous morphology showed to be hugely beneficial in accommodating cells, thus providing the potential to incorporate drugs, growth factors and other biological components with the aim to release on demand.<sup>26</sup>

Furthermore, recent studies have evaluated the biocompatibility and osteogenic potential of CaP microspheres mixed with autologous bone marrow concentrate (BMC) in a large animal model (sheep).<sup>27</sup> Histological results showed the formation of a collagen-enriched matrix and mineralization of the tissue within the defect after 13 weeks post-implementation, suggesting commitment toward the bone lineage. However, incorporating BMC within the CaP glass microspheres did not show any significant differences in the histology results in comparison to microspheres implanted alone. In this in-vivo study, the surgical procedure included anesthetization, creation of a cylindrical bone defect of 8 mm width x 15 mm depth into cancellous bone of

medial femoral condyles, then filling with glass microspheres loaded with autologous stem cells followed by suturing the skin. In order to reduce the use of this type of complicated and traumatic surgical intervention, a minimally invasive procedure is always preferred, such as injection of the material using a syringe in the area of interest.

In this study, the formulation, rheology, flow behavior and injectability of these porous CaP glass microspheres along with various viscosity modifiers (such as, xanthan gum, methyl cellulose and carboxyl methyl cellulose) via syringe needles (14G and 18G) has been explored. Moreover, non-porous CaP microspheres in combination with porous microspheres were also evaluated to increase the load of ions as well as to include additional mechanical load bearing support in the formulation paste. Thus, this CaP formulation paste can be combined with cell-based therapies that would allow injecting them via a small hole into the bones of those at risk of fracture to provide a localized increase in bone density.

## **2. Materials and methodology**

### **2.1. Microsphere manufacture**

The microspheres consisted of calcium phosphate-based glass formulation 40 P<sub>2</sub>O<sub>5</sub> - 16 CaO - 24 MgO - 20 Na<sub>2</sub>O (in mol%). They were prepared via melting quenching process using precursors NaH<sub>2</sub>PO<sub>4</sub>, CaHPO<sub>4</sub>, MgHPO<sub>4</sub> and P<sub>2</sub>O<sub>5</sub>. The glass produced was further processed to achieve porosity (or non-porosity) and spherical morphology using a flame spheroidization process.<sup>18</sup> Morphology of the CaP glass microspheres was determined using scanning electron microscope (SEM). The CaP glass microspheres were imaged under low vacuum without a coating using a FEI

Quanta 650 environmental scanning electron microscope (Oxford Instruments INCA 350 EDX system/80mm X-Max SDD detector, EBSD and KE Centaurus EBSD system). Porosity ( $\phi$ ) was calculated from the absolute density ( $\rho_{\text{abs}}$ , helium gas pycnometer method) and apparent density ( $\rho_{\text{app}}$ , mass in 10 mL cylinder) using Eq 1.<sup>28,29</sup>

$$\phi = (\rho_{\text{abs}} - \rho_{\text{app}}) / \rho_{\text{abs}} \quad \text{Eq 1}$$

## 2.2. Preparation of microsphere pastes (injectable technology)

CaP glass microsphere pastes were prepared using two particle size ranges (60-125  $\mu\text{m}$  and 125-200  $\mu\text{m}$ ) of gamma sterilized porous and non-porous microspheres. In this work the main interest was to test the injectability of porous microspheres to allow the transport of stem cells inside the porous; however, some tests were also performed with the inclusion of non-porous microspheres to increase the concentration of ions. We used cell culture media (DMEM Dulbecco's Modified Eagle, ThermoFisher Scientific) for the data presented in this paper; however, we also tested the optimal formulation with saline solution (0.9% NaCl) to evaluate if the flow behavior was maintained. To formulate an injectable CaP glass microsphere paste, it was necessary to use aqueous compatible excipients to mediate the delivery of this new glass material. We tested gamma sterilized xanthan gum (XG, Sigma-Aldrich), sodium carboxyl methyl cellulose (CMC, MW 250000 (DS=0.7), Acros Organics) and methyl cellulose (MC, Sigma-Aldrich). They were selected from a list of ten candidates based on their viscosity and elasticity properties when dispersed in solution; however, their stability as a function pH and temperature were also considered.<sup>30-33</sup> Sterilization was achieved using gamma irradiation (Cobalt 60, dose 25-35 kGy) as a standard procedure in orthopedics. Furthermore, we also tested hyaluronic acid (HA, MP Biomedicals) and polyethylene glycol (PEG<sub>8000</sub>, Alfa

Aesar). However, as both HA and PEG failed to improve the flow properties of the paste, they were discarded during preliminary tests. To date, any of these excipients have not been tested in humans; however, XG has been injected in rabbits and rats to treat osteoporosis conditions.<sup>34-35</sup>

The formulations were tested and optimized, the loading of solids in the carrier solution (solid to liquid ratio, S/L) were quantified as grams per milliliter (g/mL).

### 2.3. Rheology

The rheological characteristics of the microsphere pastes were assessed through measurements of viscosity and viscoelasticity using a rheometer (Kinexus Pro, Malvern Instruments). For the viscosity measurements, excipient solutions in DMEM were evaluated at concentrations between 20 and 80 mg/mL. Pastes composed of CaP glass microspheres (60-125  $\mu\text{m}$ , 125-200  $\mu\text{m}$  or a mixture of both size ranges), with DMEM, and excipient were also evaluated for viscosity. All viscosity measurements were performed at 20°C.

The viscoelasticity was monitored through examining the elastic component ( $G'$ ), viscous component ( $G''$ ) and phase angle ( $\delta$ ).  $G'$  relates to the degree of elasticity of the material whereas  $G''$  measures the degree of viscosity. The crossover point provides a measure of the point where behavior switches from liquid-like to solid-like properties. The rheometer was used in oscillatory mode and a sinusoidal shear stress was applied to the microsphere pastes to measure deformation. Using this approach, a strain sweep was first performed to determine the linear region of viscoelasticity (LVER), then the limit of LVER was used to perform a frequency sweep test in which  $G'$  and  $G''$  were quantified as a function of angular frequency ( $\omega$ ). The systems evaluated for viscoelasticity consisted of CaP glass microspheres

(125-200  $\mu\text{m}$ ), DMEM and excipient. The measurements were performed at 20°C and 37°C to mimic conditions of injection and post-injection.

#### 2.4. Injection of microsphere pastes

Luer-lock syringes of 3, 5, 10 and 20 mL (BD™ Pastipak™ of internal diameter 8.66 mm, 12.06 mm, 14.5 mm, 19.13 mm, respectively) were connected to either a 14G needle (1.6 mm internal diameter by 15 mm length) or 18G needle (0.84 mm internal diameter by 15 mm length). The microsphere pastes were prepared according to the formulations previously defined and loaded into the syringes. Trapped air was effectively removed using a locking syringe plunger whilst flicking the syringe. The syringes were mounted for extrusion in a compression tester (Instron 5566 Test Bench). The force (N) required for the extrusion of the paste was determined over a plunger displacement of 20 mm at a rate of 20 mm/min. The pressure (MPa) was calculated by dividing the force (N) by the cross section of the area ( $\text{mm}^2$ ) of the syringe.

### 3. Results

#### 3.1. Microsphere characteristics

SEM analyses showed the random and interconnected porosity of the CaP glass microspheres with a wide distribution of pore sizes (Figs. 1a and 1b). Non-porous glass microspheres are also shown in Fig 1c.



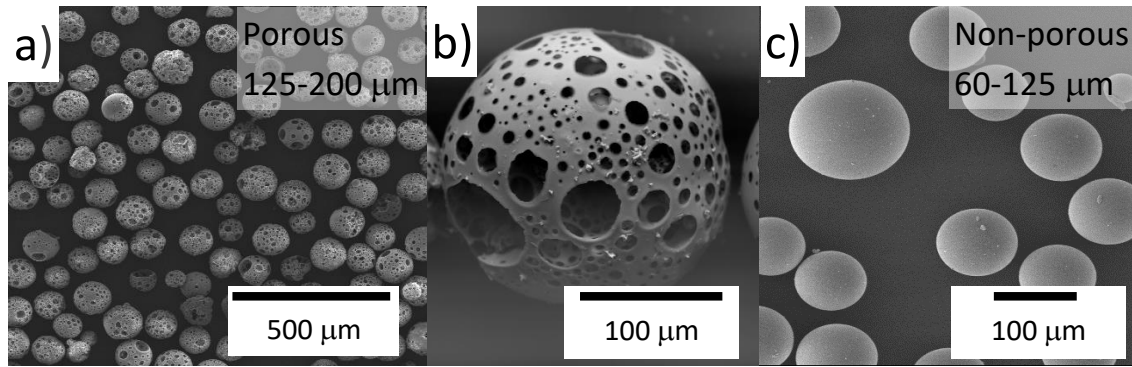


**Fig. 1.** a) SEM image showing the as-synthesized porous CaP glass microspheres (125-200  $\mu\text{m}$ ); b) Detail of the interconnected porosity of the glass microspheres; c) Non-porous CaP glass microspheres (60-125  $\mu\text{m}$ ).

Density measurements indicated that the absolute density of the CaP glass microspheres was  $2.52 \pm 0.02 \text{ g.cm}^{-3}$  and the apparent density was  $0.70 \pm 0.05 \text{ g.cm}^{-3}$ . The calculated porosity of the microspheres using Eq 1 was found to be  $75 \pm 3\%$ , which was very similar to the porosity value obtained for these porous microspheres by mercury porosimetry ( $76 \pm 5\%$ ) previously reported by Hossain et al., 2018.<sup>18</sup>

### 3.2. Paste characteristics

CaP glass microsphere pastes extruded through a needle formed with and without excipient are shown in Fig. 2. Glass microsphere pastes without excipient were extremely difficult to extrude, and during injection developed a filter cake condition in which the microspheres interlocked and the surrounding fluid emerged first (Fig. 2a). This condition allowed an extrusion of a small amount of paste by using significant force (300 N). Better paste consistency and flow enhancement was observed when using excipients (XG, MC, and CMC) in DMEM. It allowed the extrusion of the glass microsphere paste through small syringes (1 and 3 mL) and small needles (14G, 18G) with forces small enough to allow extrusion by hand (Figs. 2b and 2d). Similar flow characteristics were obtained when using saline solution (0.9% NaCl) instead of

DMEM. Mixtures containing hyaluronic acid and PEG<sub>8000</sub> failed to form an injectable paste and were discarded for further study (Figs. 2e and 2f).

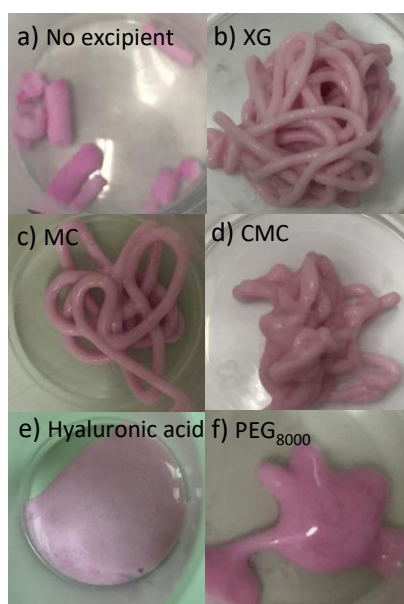


**Fig. 2.** CaP glass microsphere pastes formed a) no excipient, filter cake is formed; b) DMEM and XG; c) DMEM and MC; d) DMEM and CMC; e) DMEM and hyaluronic acid and f) DMEM and PEG<sub>8000</sub> respectively yielding a slurry instead of a paste. In all the tests, delivery was performed through a standard 3 mL syringe and a 14G needle (8.66 mm and 1.6 mm internal diameter respectively).

Scanning electron microscope (SEM) images of the CaP glass microspheres were collected with and without XG to observe the effect of adding the excipient. The images were collected after injection using a 3 mL syringe and a 14G needle (8.66 mm and 1.6 mm internal diameter respectively). The injection without XG experienced a filter cake condition that contributed to the breakdown of the porous CaP glass microspheres (Fig. 3a). However, the use of 40 mg/mL of XG prevented the microspheres from damage increasing viscosity and improving the flow of the formed paste (Fig. 3b). High resolution images of the wet paste, injected and carefully removed from the 3D lattice (0.95 mm x 0.95 mm x 1.0 mm), showed that

the CaP glass microspheres remained agglomerated together as a single structure with a small amount of XG (Fig. 3c).

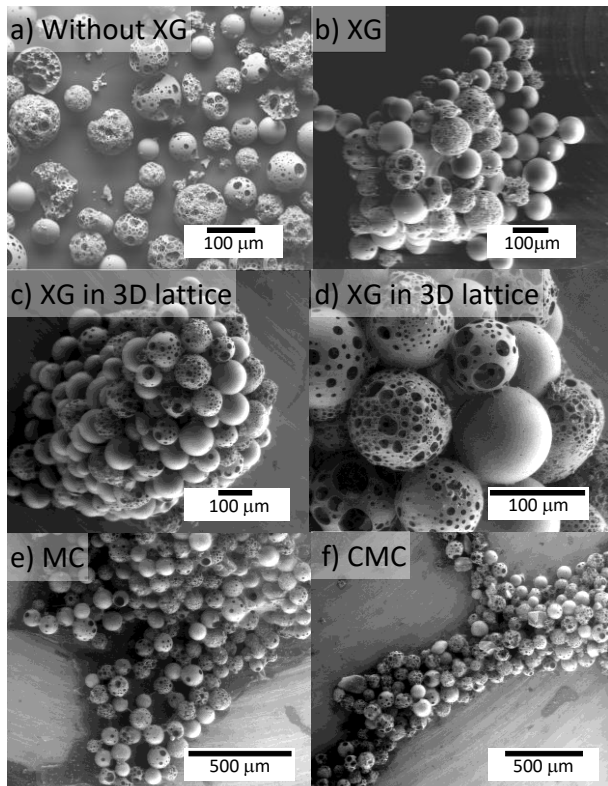


**Fig. 3.** Extruded pastes through a 3 mL syringe and 14G needle a) without XG; b) with XG; c) and d) with XG after testing into a 3D osteoporotic lattice (0.95 mm x 0.95 mm x 1.0 mm dimensions); e) Porous CaP glass microsphere pastes prepared with MC and d) with CMC. The images were collected in wet pastes without further preparation using an environmental SEM.

Early tests showed that MC and CMC imparted similar flow behavior to the glass microsphere pastes as with XG; however, those containing CMC lost structure and shape within four hours of the test, making CMC unfavorable candidate for injection and delivery. Therefore, only MC was carried forward for evaluation alongside XG. The required concentration of excipient was estimated through viscosity measurements with solutions at different concentrations (Figs. 4a and 4b). Among all the solutions, those containing XG showed the highest viscosity at rest; however,

the viscosity rapidly decreased with the increase of shear rate presenting a shear thinning behavior (Fig. 4a). At any given shear rate, the solutions with 40 and 60 mg XG per mL of DMEM had the highest viscosities; however, when 60 mg/mL was used, partial dissolution of XG in the liquid media was observed limiting its concentration to below this value. The viscosity also increased progressively with the concentration of MC solutions (40, 60 and 80 mg/mL) but to a lower extent than XG solutions.

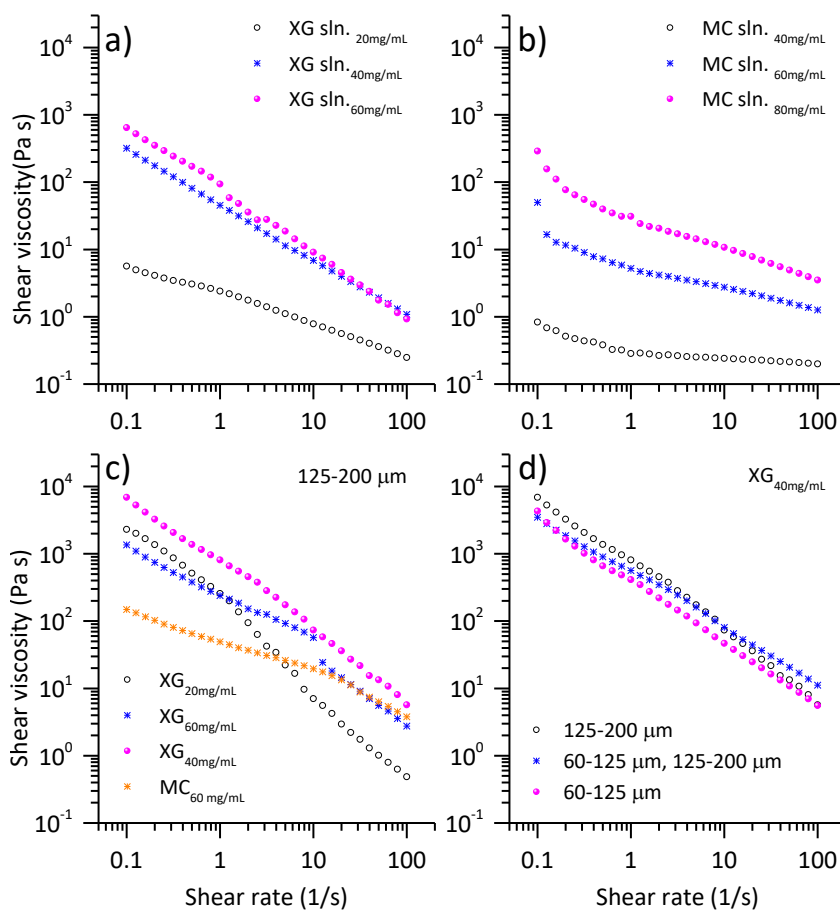


**Fig. 4.** Viscosity as a function of shear rate of (a) XG solutions (concentrations between 20 and 60 mg/mL), and (b) MC solutions (concentrations between 40 and 80 mg/mL) in DMEM; (c) Viscosity of pastes formed with CaP glass microspheres (0.48g/mL of DMEM) of 125-200  $\mu\text{m}$  in DMEM with either XG or MC as an excipient; (d) Viscosity of microsphere pastes using different size range of CaP glass

microspheres formed with 40 mg/mL of XG and DMEM solutions. All measurements were performed at 20°C.

Similar tests were performed with CaP glass microspheres (0.48g/mL of DMEM, 125-200  $\mu$ m) and excipient solutions (either 20, 40, 60 mg/mL of XG, 60 mg/mL of MC). Consistently, the results indicated that microsphere pastes containing XG had higher viscosities, in particular at low shear rate forming a solid-like paste at rest (Fig. 4c). The best performance was obtained when using 40mg/mL of XG which provided excellent injectability and ensured full hydration of the XG (Fig. 4d).

Nevertheless, the viscoelasticity of glass microsphere pastes consisting of 40 mg/mL of XG and 60 mg/mL of MC were further evaluated at 1Hz at 20°C. The viscoelasticity results indicated that the elastic component ( $G'$ ) dominated between 0.001 and 10% shear rate in CaP glass microsphere pastes containing 40 mg/mL of XG. They had high  $G'$  values (~27000- 29000 Pa, Figs. 5a and 5c) and low phase angle values ( $\delta=10-30^\circ$  at 20°C) suggesting that XG containing pastes had a strong structure (Figs. 5a and 5c). These results were also consistent at 37°C in which the elastic component ( $G'$ ) dominated across low and high frequencies indicating that the glass microsphere pastes behaved as a viscoelastic solid-like material (see Figs. 5b and 5d). Furthermore, evaluation of the system using 40mg/mL of XG at 20°C and 1Hz showed that the linear viscoelastic region extended to a strain of 0.02 %; after this value, the structure of the microsphere paste started to change. The solid-like behavior and higher elasticity make this system very effective as a filler and its characteristics were maintained when the system was exposed to 37°C.

In contrast, glass microsphere pastes prepared with 60 mg/mL of MC showed low stiffness ( $G' \sim 1300-400$  Pa, Figs. 6a and 6c) in comparison to XG containing pastes.

The phase angle ( $\delta$ ) values were found to be between 20 and 60° indicating a liquid-like (viscous) behavior (Figs. 6a and 6c). This performance was even more evident at 37°C as the system showed a linear viscoelastic region up to 0.39% in strain in comparison to 0.01 % at 20°C. This indicated that although the microsphere paste prepared with MC could behave as a solid-like material at 20°C, it may flow at rest when exposed to 37°C.

In addition, stability of the pastes were evaluated by immersing them in DI water for 24 hours. The results indicated that XG pastes hydrated but conserved the shape after this time, and even the shape was still visible after 48 hours; however, pastes formed with MC flattened after 1 hour of immersion and fully dispersed after the 24 hour period.

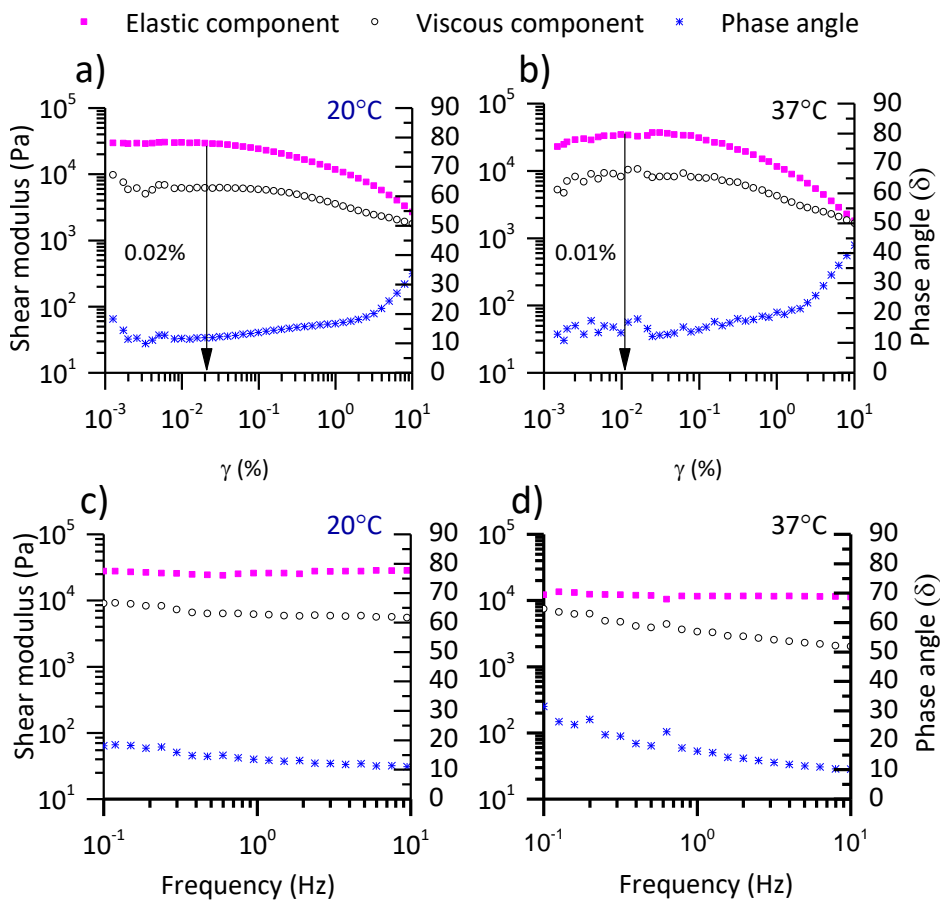


**Fig. 5.** Elastic component  $G'$ , viscous component  $G''$ , and phase angle  $\delta$  as a function of shear stress for the pastes containing 125-200  $\mu\text{m}$  CaP glass microspheres in DMEM and XG evaluated at 1Hz frequency at (a) 20°C and (b) 37°C.  $G'$ ,  $G''$ , and  $\delta$  as a function of oscillatory frequency for similar glass microsphere pastes at (c) 20°C and (d) 37°C.

Overall, since the role of the carrier medium was to maintain a suspension of the glass microspheres (i.e. high viscosity) and then upon delivery the role was to resist shear forces to minimize transport away from the delivery site, the viscoelastic properties observed with XG proved to be highly beneficial for the flow characteristics of the glass microsphere paste, thereby enabling minimally invasive treatment opportunities utilizing small needles. As such, XG was the excipient chosen for further investigation.

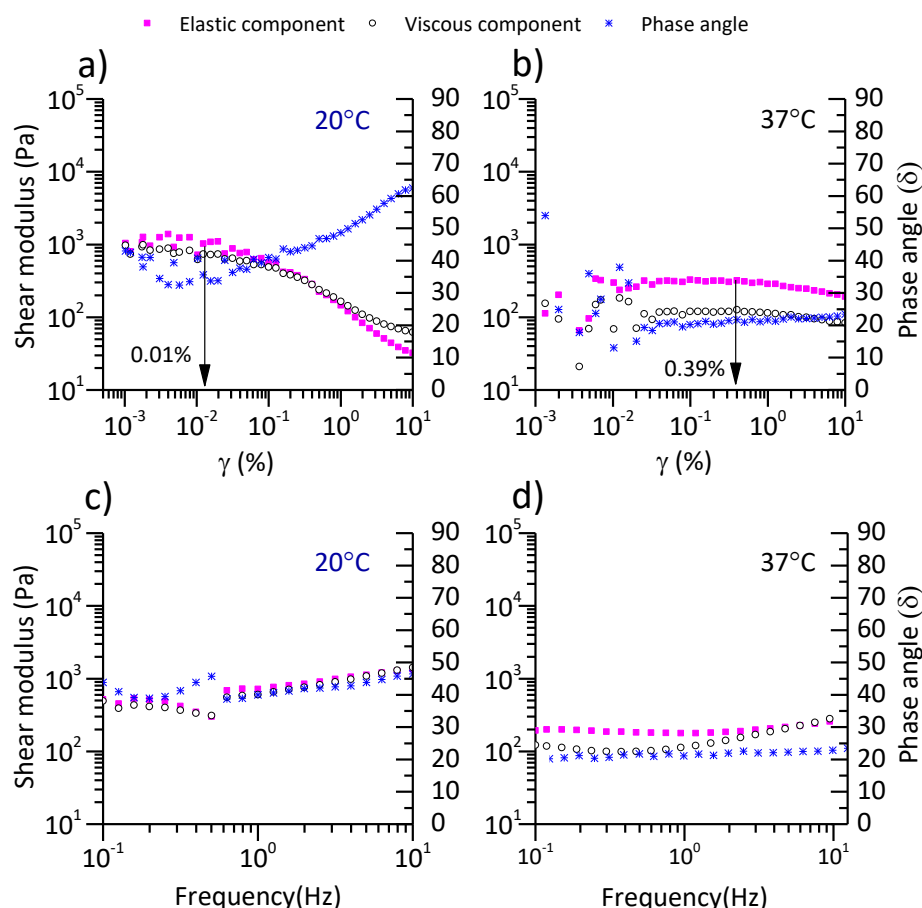


**Fig. 6.** Elastic component  $G'$ , viscous component  $G''$ , and phase angle ( $\delta$ ) as a function of shear stress for the systems composed of microsphere pastes (125-200  $\mu\text{m}$ ) in DMEM and MC at (a) 20°C and (b) 37°C.  $G'$ ,  $G''$ , and  $\delta$  as a function of oscillatory frequency for similar glass microsphere pastes at (c) 20°C and (d) 37°C.

### 3.3. CaP glass microsphere paste formulation

The properties of the microsphere paste were also evaluated by combining porous and non-porous CaP glass microspheres of similar size-range together, and by also mixing porous microspheres between the two size ranges. The base formulation was first formed using the initial formulation for porous CaP glass microspheres (1g of 60-125  $\mu\text{m}$  or 0.48g 125-200  $\mu\text{m}$ ) and mixed with 0.04g of gamma sterilized XG and 1 mL of DMEM. The amount of porous CaP glass microspheres was systematically reduced and replaced by non-porous (solid) glass microspheres to form a paste of



similar consistency. A plot of the weight of porous and non-porous CaP glass microspheres to obtain the injectable paste followed an inverse linear relationship in which 0.10 g of porous microspheres could be replaced by 0.60 g of non-porous microspheres (Figs. 7a and 7b). In all cases, to the right of the hatched box shows failure due to a high solid loading and filter pressing, and to the left of the hatched box shows the region in which the pastes have poor structure; neither are injectable (Fig. 7a) The hatched region indicates a successful combination of porous and non-porous CaP glass microspheres (Figs. 7a and 7b).

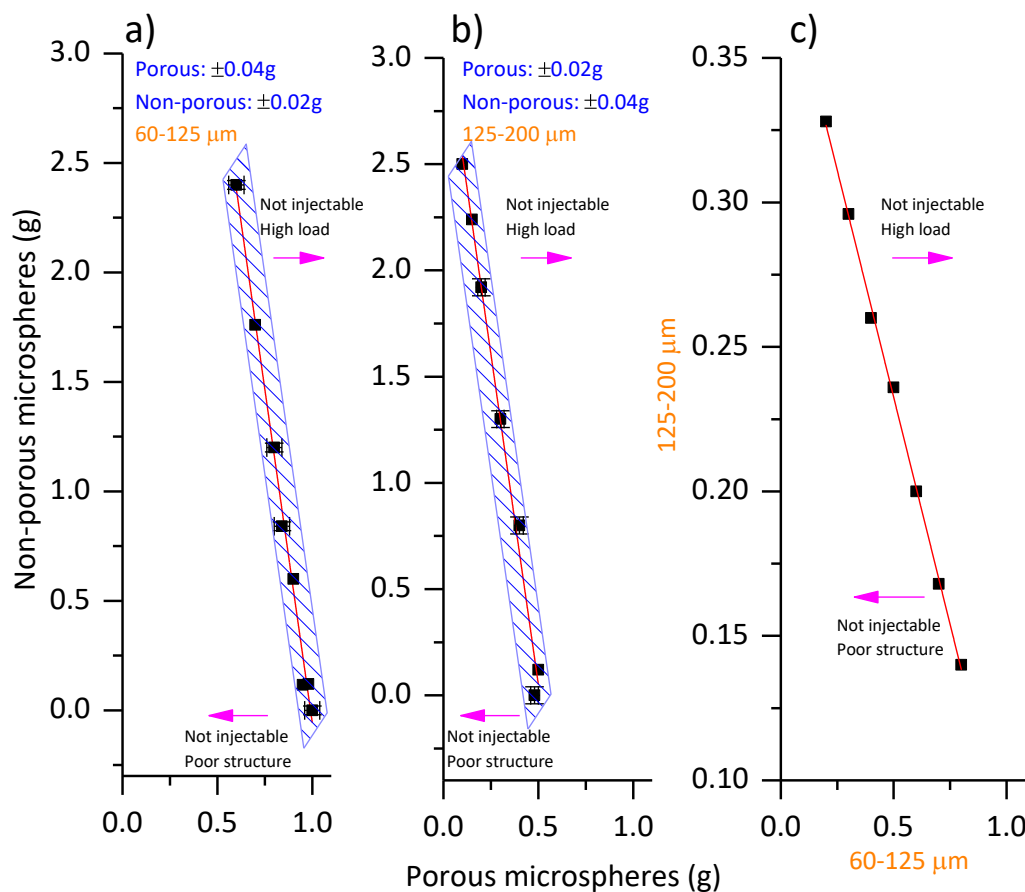


**Fig. 7.** (a) Established formulations for injectable microsphere pastes using a combination of porous and non-porous with particle sizes between 60-125  $\mu\text{m}$  using 1 mL DMEM and 0.04g gamma sterilized XG; (b) as before but using particle sizes

between 125-200  $\mu\text{m}$ ; and (c) porous CaP glass microspheres using a mixture of sizes (60-125  $\mu\text{m}$  and 125-200  $\mu\text{m}$ ).

The successful combination achieved with porous two screened glass microsphere sizes (60-125  $\mu\text{m}$  and 125-200  $\mu\text{m}$ ) CaP glass microspheres is shown in Fig. 7c. The established formulations were plotted as a function of solid to liquid ratios (S/L, Fig. 8). High S/L ( $> 1 \text{ g/mL}$ ) were achieved by using a higher proportion of non-porous glass microspheres regardless the size range used; however, the formulations with only porous CaP glass microspheres for the inclusion of stem cells will yield lower S/L (Fig. 8a).

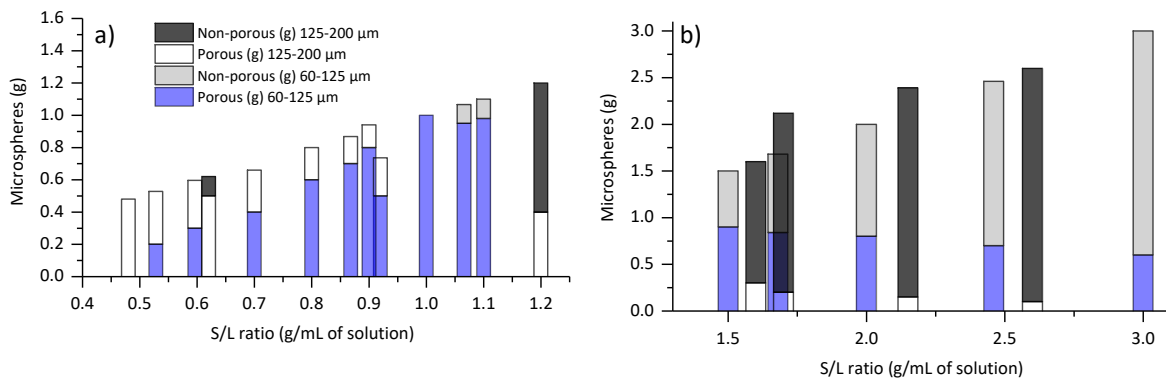


**Fig. 8** Injectable formulations containing porous and non-porous CaP glass microspheres as a function of the S/L ratio (g/mL of solution); a) low S/L ratios (0.4 to 1.3 g/mL) obtained mainly through the combination of porous microspheres; b) high ratios (1.5 to 3.0 g/mL) obtained when non-porous spheres are introduced in the formulation.

### 3.4. Injection pressure

The pressures for extrusion of microsphere pastes containing XG, CaP (0.48 g, 125-200  $\mu\text{m}$ ) and DMEM (1 mL), were quantified between 0.3 and 0.5 MPa using syringes of 3, 10 and 20 mL (Fig. 9a). Similar pressures ( $< \sim 0.4 \text{ MPa}$ ) were required to extrude

pastes of all formulations tested, and even when using different range size of microspheres (Figs. 9b-9d). These pressures are low enough to inject the pastes by hand without any need of a special device to aid with the pressure of system. The low pressures required to extrude the pastes were only possible with the addition of XG to the mixture, without XG the pressures reached 300MPa to extrude 30% of the paste before the syringe failed. A more detailed discussion regarding pressures as a function of load are not applicable to the glass pastes studied in this work because the material is not homogeneous in size and the microspheres have different porosities; these factors make a different structure in every batch. Nevertheless, the use of XG made possible to reduce the pressures to inject by hand without noticing a difference in behavior during injection acting as a modifier of the rheological properties of the CaP glass.

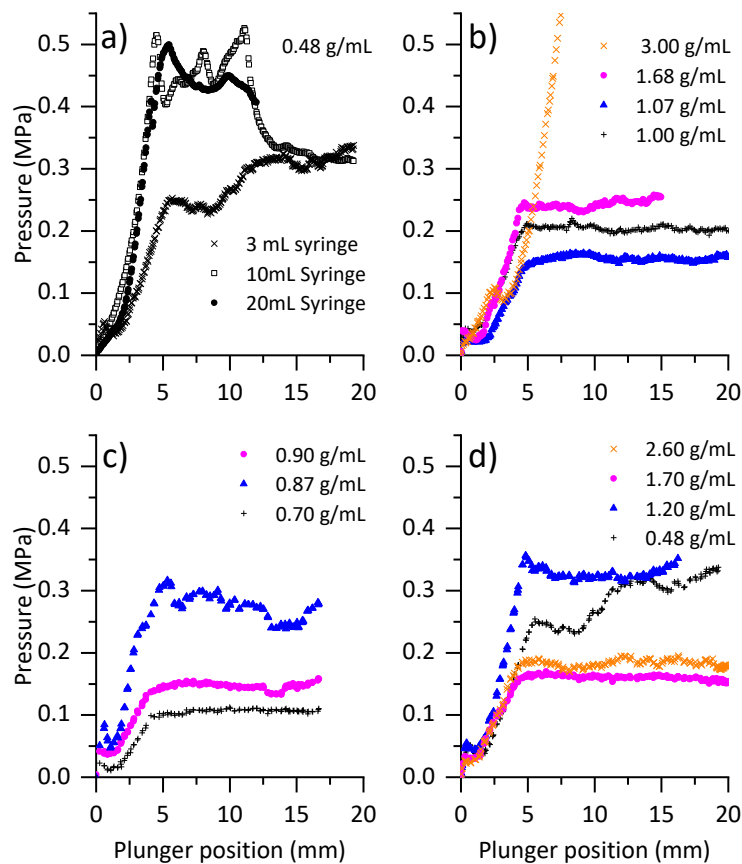


**Fig. 9.** (a) Total pressure required to extrude the microsphere paste using 0.48g/mL and 125-200  $\mu\text{m}$  CaP glass microspheres through 3, 10 and 20 mL syringes and a 14G needle; in all three cases the pressures were below 0.5 MPa; (b) total pressure to extrude porous and non-porous microsphere pastes (60-125  $\mu\text{m}$ ) using 3 mL syringes; c) total pressure required to extrude porous microsphere pastes (60-125  $\mu\text{m}$  and 125-200  $\mu\text{m}$ ) using 3 mL syringes; d) total pressure required to extrude porous and non-porous microsphere pastes (125-200  $\mu\text{m}$ ) using 3 mL syringes.

#### 4. Discussion

Recent developments in bone regeneration have shifted towards orthobiologics, where one of the approaches explores the use of cell therapy treatments which involves the utilization of novel emerging biomaterials with the capability to accommodate stem cells, whilst also contributing essential elements for bone formation and repair.<sup>36,37</sup> Porous microspheres constitute an effective material to fulfil these needs and tunable porous CaP glass microspheres have recently been produced for the first time.<sup>18</sup> As-synthesized and mixed with simple DMEM, these porous microspheres are not injectable as they require high forces ( $>300\text{N}$ ) for extrusion and the formation of a filter cake within the injection device does not allow delivery of the intended formulation. Addition of xanthan gum (XG) to the CaP glass microsphere paste dispersed in liquid media (either DMEM or saline solution), increased the viscosity and imparted elasticity to form a paste that ultimately improved its flow characteristics and facilitated injection and delivery. This improvement was maintained at both room and body temperature. Similarly, methyl cellulose (MC) and carboxyl methyl cellulose (CMC) also improved the flow properties of the glass microsphere paste, however, the resulting paste was found to behave predominantly as a viscous-liquid, prone to dispersion from the place of injection, in particular at body

temperature (Figs. 5c and 5d). Previous studies have demonstrated that viscosity is a key factor that determines flow of filling materials,<sup>38-41</sup> however this study showed that the increase of viscosity alone does not improve the flow behavior of porous CaP glass microspheres. Other factors such as particle size distribution and the intrinsic surface area can also affect the viscosity and the flow characteristics.

The glass microsphere paste formulations prepared with XG were able to be extruded from standard syringes in the range of 3 to 20 mL using relatively small diameter needles (14G and 18G). Furthermore, the addition of XG into the system prevented the CaP glass microspheres from damage during delivery (Figs 3c and 3d) as the injection pressure was reduced to less than 0.5 MPa. The optimum behavior was achieved when using 40 mg/mL of XG; below this concentration the microsphere-media mixture showed poor structure and showed formation of a filter cake in common with the formulation not including XG.

The formation of a paste prepared with porous CaP glass microspheres was greatly affected by the presence of non-porous microspheres. As such, the formulations to make an injectable paste were restricted to specific proportions between non-porous and porous CaP glass microspheres. Injectable formulations which combined porous and non-porous CaP glass microspheres followed a linear relationship given by  $\text{mass}_{\text{non-porous}} = 6 \times \text{mass}_{\text{porous}}$  (within  $\pm 0.02$  g in weight). This relationship was related to the density of the particles as the volume fraction was maintained constant (i.e., the density of the non-porous particles is ~ 6 times higher than the porous particles). The porous CaP glass microspheres allowed greater fluid volume to be carried (i.e. within the internal structure of the particles) whilst maintaining an efficient formulation for delivery (i.e. both injectable and with structural properties in absence of flow). The presence of non-porous CaP glass microspheres in the

formulation increased the solid to liquid ratio from 1.0 g/mL to 3.0 g/mL (i.e. 10% non-porous 1.5 g/mL; 20% non-porous 2.0 g/mL; 40% non-porous 3.0 g/mL). This is important because non-porous CaP glass contributes to a higher concentration of biotherapeutic ions (e.g.,  $\text{Ca}^{2+}$ ,  $\text{Mg}^{2+}$ ) that could potentially play important roles during the bone repair and regeneration process.<sup>42</sup> This also allows tuning of the overall formulation to provide structural rigidity and a source of ions whilst carrying cells (and or other biological entities), depending on the particular end application. In addition, having non-porous CaP glass microspheres as a result of a manufacturing process, no more than 8% from the total mass of the batch of microspheres should be solid to be injectable.

The size range of the particles also affected the formulation of the microsphere pastes. For 1mL of either DMEM a successful composition consisting of 1g of 60-125  $\mu\text{m}$  or 0.48g of 125-200  $\mu\text{m}$  of CaP glass microspheres was required to maintain the ideal consistency of the paste for delivery. This indicated that the larger CaP glass microspheres required twice the volume of solution to form the paste than the smaller microspheres, suggesting that increasing the proportion of larger microspheres in the formulation, would decrease the S/L ratios. Conversely, the use of only porous microspheres would yield lower solid to liquid ratios.

During the injection process, the pressure rapidly increased at the beginning of the injection; however, it was maintained below 0.5 N/mm<sup>2</sup> providing good flow, even when using large syringes (10-20 mL) and small needles (14G and 18G). The pressure profiles of injecting CaP glass microsphere pastes evaluated here, showed the same trend as those presented in previous works for irregular shaped calcium phosphate materials, in which the pressure rapidly increased reaching a steady state as the extrusion of the paste progressed.<sup>43</sup> Our study demonstrated that the increase of

viscosity does not necessarily improve the flow characteristics of the porous CaP glass microsphere, at least with their composition and morphology, but particle size, surface area and in particular, the elastic component imparted by XG played a significant role. This is contradictory to the reported injectability of similar CaP glass materials in which an increase in viscosity increases injectability;<sup>43</sup> however, in this work that behavior was not observed as demonstrated with our results using MC in which only the viscosity is increased. Instead, the elasticity and viscosity of XG allowed the porous CaP microspheres to form an injectable paste. These characteristics in-turn impart restrictions on the S/L ratio restricting the formulation. Overall, the addition of XG in the optimal concentration produced a robust CaP microsphere paste, which could deliver microspheres without damage easily via simple injection through small < 2mm inner diameter needles.

## **5. Conclusions**

Porous and non-porous CaP glass microspheres synthesized for cell-based bone regeneration treatment were found to be injectable when excipient was added. From the excipients evaluated, xanthan gum provided the best flow characteristics compared to methyl cellulose and carboxyl methylcellulose at room and body temperature. The extrusion of paste was achieved using 14G and 18G needles and syringe in sizes from 3 to 20 mL. The use of xanthan gum protected the porous CaP glass microspheres from damage during injection due to its viscoelastic properties. Formulation of porous CaP glass microspheres for delivery in paste form must follow specific ratios and adjustments must be made when non-porous microspheres are present. Flow characteristics of the glass microsphere paste in media (i.e. DMEM or saline solution) depend on particle size, surface area, S/L ratio, and concentration of excipient that provides viscoelastic properties. Overall, a formulation with xanthan

gum as an excipient to porous CaP glass microspheres allowed for effortless delivery through narrow diameter needles.

## Acknowledgements

This paper summarizes independent research funded by the National Institute for Health Research (NIHR) under its i4i Challenge Award Programme (Grant Reference Number: II-C3-0714-20001). The views expressed are those of the authors and not necessarily those of the NHS, the NIHR or the Department of Health. The authors would also like to acknowledge Tony Wiese and for his support during force measurements. Also, we would like to thank Ceramisys Limited (UK) for their kind contribution to gamma sterilization studies.

## References

1. Svedbom, A.; Hernlund, E.; Ivergård, M.; Compston, J.; Cooper, C.; Stenmark, J.; McCloskey, E. V.; Jönsson, B.; Kanis, J. A.; IOF, E. U. R. P. o., Osteoporosis in the European Union: a compendium of country-specific reports. *Archives of osteoporosis* 2013, 8 (1-2), 137-137. DOI: 10.1007/s11657-013-0137-0.
2. Van Staa, T. P.; Dennison, E. M.; Leufkens, H. G. M.; Cooper, C., Epidemiology of fractures in England and Wales. *Bone* 2001, 29 (6), 517-522. DOI: [https://doi.org/10.1016/S8756-3282\(01\)00614-7](https://doi.org/10.1016/S8756-3282(01)00614-7).
3. Prodovic, T.; Ristic, B.; Rancic, N.; Bukumiric, Z.; Zeljko, S.; Ignjatovic-Ristic, D., Factors Influencing The Six-Month Mortality Rate In Patients With A Hip Fracture: dejavniki, ki vplivajo na šestmesečno stopnjo umrljivosti pri bolnikih z zlomom kolka. *Zdravstveno varstvo* 2016, 55 (2), 102-107. DOI: 10.1515/sjph-2016-0015.



4. Kilci, O.; Un, C.; Sacan, O.; Gamli, M.; Baskan, S.; Baydar, M.; Ozkurt, B., Postoperative Mortality after Hip Fracture Surgery: A 3 Years Follow Up. *PLOS ONE* 2016, 11 (10), e0162097. DOI: 10.1371/journal.pone.0162097.
5. Johnell, O.; Kanis, J. A., An estimate of the worldwide prevalence and disability associated with osteoporotic fractures. *Osteoporosis International* 2006, 17 (12), 1726-1733. DOI: 10.1007/s00198-006-0172-4.
6. Shibamoto, A.; Ogawa, T.; Duyck, J.; Vandamme, K.; Naert, I.; Sasaki, K., Effect of high-frequency loading and parathyroid hormone administration on peri-implant bone healing and osseointegration. *International Journal of Oral Science* 2018, 10 (1), 6. DOI: 10.1038/s41368-018-0009-y.
7. Hawley, S.; Leal, J.; Delmestri, A.; Prieto-Alhambra, D.; Arden, N. K.; Cooper, C.; Javaid, M. K.; Judge, A.; Group, f. t. R. S., Anti-Osteoporosis Medication Prescriptions and Incidence of Subsequent Fracture Among Primary Hip Fracture Patients in England and Wales: An Interrupted Time-Series Analysis. *Journal of Bone and Mineral Research* 2016, 31 (11), 2008-2015. DOI: doi:10.1002/jbmr.2882.
8. Järvinen, T. L.; Michaëlsson, K.; Jokihaara, J.; Collins, G. S.; Perry, T. L.; Mintzes, B.; Musini, V.; Erviti, J.; Gorricho, J.; Wright, J. M.; Sievänen, H., Overdiagnosis of bone fragility in the quest to prevent hip fracture. *BMJ : British Medical Journal* 2015, 350, h2088. DOI: 10.1136/bmj.h2088.
9. Lim, S. Y. B., Marcy B, Current approaches to osteoporosis treatment. *Current Opinion in Rheumatology* 2015, 27 (3), 216-224.
10. Reginster, J.-Y., Antifracture Efficacy of Currently Available Therapies for Postmenopausal Osteoporosis. *Drugs* 2011, 71 (1), 65-78. DOI: 10.2165/11587570-000000000-00000.

11. Klop, C.; Gibson-Smith, D.; Elders, P. J. M.; Welsing, P. M. J.; Leufkens, H. G. M.; Harvey, N. C.; Bijlsma, J. W. J.; van Staa, T.-P.; de Vries, F., Anti-osteoporosis drug prescribing after hip fracture in the UK: 2000–2010. *Osteoporosis International* 2015, 26 (7), 1919-1928. DOI: 10.1007/s00198-015-3098-x.
12. Weglein, A.; Sampson, S.; Aufiero, D., Platelet Rich Plasma Practical Use in Non-Surgical Musculoskeletal Pathology. In Platelet-Rich Plasma: Regenerative Medicine: Sports Medicine, Orthopedic, and Recovery of Musculoskeletal Injuries, Lana, J. F. S. D.; Andrade Santana, M. H.; Dias Belangero, W.; Malheiros Luzo, A. C., Eds. Springer Berlin Heidelberg: Berlin, Heidelberg, 2014; pp 187-201. DOI: 10.1007/978-3-642-40117-6\_8.
13. Sampson, S.; Bemden, A. B.-v.; Aufiero, D., Autologous Bone Marrow Concentrate: Review and Application of a Novel Intra-Articular Orthobiologic for Cartilage Disease AU - The Physician and Sportsmedicine 2013, 41 (3), 7-18. DOI: 10.3810/psm.2013.09.2022.
14. Toolan, B. C., Current Concepts Review: Orthobiologics. *Foot & Ankle International* 2006, 27 (7), 561-566. DOI: 10.1177/107110070602700715.
15. Caplan, A.I., Mesenchymal stem cells. *Journal of Orthopaedic Research* 1991, 9, 641-650.
16. Kwon, S.G., Kwon, Y.W., Lee, T.W., Park, G.T., Kim, J.H., Recent advances in stem cell therapeutics and tissue engineering strategies. *Biomaterials Research* 2018, 22, 36.
17. Zhang, Y., Grosfeld, E.C., Camargo, W.A., Tang, H., Magri, A.M.P., van den Beucken, J.J.J.P., Efficacy of intraoperatively prepared cell-based constructs for bone regeneration. *Stem Cell Research & Therapy* 2018, 9, 283.

18. Hossain, K. M. Z.; Patel, U.; Kennedy, A. R.; Macri-Pellizzeri, L.; Sottile, V.; Grant, D. M.; Scammell, B. E.; Ahmed, I., Porous calcium phosphate glass microspheres for orthobiologic applications. *Acta Biomaterialia* 2018, 72, 396-406. DOI: <https://doi.org/10.1016/j.actbio.2018.03.040>.
19. Mitragotri, S.; Burke, P. A.; Langer, R., Overcoming the challenges in administering biopharmaceuticals: formulation and delivery strategies. *Nature Reviews Drug Discovery* 2014, 13, 655. DOI: 10.1038/nrd4363  
<https://www.nature.com/articles/nrd4363#supplementary-information>.
20. Abou Neel, E. A.; Ahmed, I.; Pratten, J.; Nazhat, S. N.; Knowles, J. C., Characterisation of antibacterial copper releasing degradable phosphate glass fibres. *Biomaterials* 2005, 26 (15), 2247-2254. DOI: <https://doi.org/10.1016/j.biomaterials.2004.07.024>.
21. Bitar, M.; Salih, V.; Knowles, J. C.; Lewis, M. P., Iron-phosphate glass fiber scaffolds for the hard–soft interface regeneration: The effect of fiber diameter and flow culture condition on cell survival and differentiation. *Journal of Biomedical Materials Research Part A* 2008, 87A (4), 1017-1026. DOI: doi:10.1002/jbm.a.31855.
22. Lakhkar, N. J.; Abou Neel, E. A.; Salih, V.; Knowles, J. C., Strontium oxide doped quaternary glasses: effect on structure, degradation and cytocompatibility. *Journal of Materials Science: Materials in Medicine* 2009, 20 (6), 1339. DOI: 10.1007/s10856-008-3688-7.
23. Valappil, S. P.; Knowles, J. C.; Wilson, M., Effect of Silver-Doped Phosphate-Based Glasses on Bacterial Biofilm Growth. *Applied and Environmental Microbiology* 2008, 74 (16), 5228-5230. DOI: 10.1128/aem.00086-08.

24. Valappil, S.; Ready, D.; Abou Neel, E.; Pickup, D.; A O'Dell, L.; Chrzanowski, W.; Pratten, J.; Newport, R.; Smith, M. E.; Wilson, M.; Knowles, J., Controlled delivery of antimicrobial gallium ions from phosphate-based glasses. 2008; Vol. 5, p 1198-210. DOI: 10.1016/j.actbio.2008.09.019.
25. Ahmed, I.; Lewis, M.; Olsen, I.; Knowles, J. C., Phosphate glasses for tissue engineering: Part 2. Processing and characterisation of a ternary-based P<sub>2</sub>O<sub>5</sub>–CaO–Na<sub>2</sub>O glass fibre system. *Biomaterials* 2004, 25 (3), 501-507. DOI: [https://doi.org/10.1016/S0142-9612\(03\)00547-7](https://doi.org/10.1016/S0142-9612(03)00547-7).
26. Li, S.; Nguyen, L.; Xiong, H.; Wang, M.; Hu, T. C. C.; She, J.-X.; Serkiz, S. M.; Wicks, G. G.; Dynan, W. S., Porous-wall hollow glass microspheres as novel potential nanocarriers for biomedical applications. *Nanomedicine: Nanotechnology, Biology and Medicine* 2010, 6 (1), 127-136. DOI: <https://doi.org/10.1016/j.nano.2009.06.004>.
27. McLaren, J.S., Macri-Pellizzeri, L., Hossain, K.M.Z., Patel, U., Grant, D.M., Scammell, B.E., Ahmed, I., Sottile, V., 2019. Porous Phosphate-Based Glass Microspheres Show Biocompatibility, Tissue Infiltration, and Osteogenic Onset in an Ovine Bone Defect Model. *ACS Applied Materials & Interfaces* 11, 15436-15446.
28. Shah, R. B.; Tawakkul, M. A.; Khan, M. A., Comparative Evaluation of Flow for Pharmaceutical Powders and Granules. *AAPS PharmSciTech* 2008, 9 (1), 250-258. DOI: 10.1208/s12249-008-9046-8.
29. Mugoni, C.; Montorsi, M.; Siligardi, C.; Andreola, F.; Lancellotti, I.; Bernardo, E.; Barbieri, L., Design of glass foams with low environmental impact. *Ceramics International* 2015, 41 (3, Part A), 3400-3408. DOI: <https://doi.org/10.1016/j.ceramint.2014.10.127>.

30. García-Ochoa, F.; Santos, V. E.; Casas, J. A.; Gómez, E., Xanthan gum: production, recovery, and properties. *Biotechnology Advances* 2000, 18 (7), 549-579. DOI: [https://doi.org/10.1016/S0734-9750\(00\)00050-1](https://doi.org/10.1016/S0734-9750(00)00050-1).
31. Shiledar, R. R.; Tagalpallewar, A. A.; Kokare, C. R., Formulation and in vitro evaluation of xanthan gum-based bilayered mucoadhesive buccal patches of zolmitriptan. *Carbohydr Polym* 2014, 101, 1234-1242. DOI: [10.1016/j.carbpol.2013.10.072](https://doi.org/10.1016/j.carbpol.2013.10.072).
32. Talukdar, M. M.; Kinget, R., Swelling and drug release behavior of xanthan gum matrix tablets. *International Journal of Pharmaceutics* 1995, 120 (1), 63-72. DOI: [https://doi.org/10.1016/0378-5173\(94\)00410-7](https://doi.org/10.1016/0378-5173(94)00410-7).
33. Park, H.; Kim, M. H.; Yoon, Y. I.; Park, W. H., One-pot synthesis of injectable methylcellulose hydrogel containing calcium phosphate nanoparticles. *Carbohydr Polym* 2017, 157, 775-783. DOI: [10.1016/j.carbpol.2016.10.055](https://doi.org/10.1016/j.carbpol.2016.10.055).
34. Chen, Q.; Mei, X.; Han, G.; Ling, P.; Guo, B.; Guo, Y.; Shao, H.; Wang, G.; Cui, Z. Bai, Y.; Xu, F., Xanthan gum protects rabbit articular chondrocytes against sodiumnitroprusside-induced apoptosis in vitro. *Carbohydrate Polymers* 2015, 131, 363-369. DOI:[10.1016/j.carbpol.2015.06.004](https://doi.org/10.1016/j.carbpol.2015.06.004).
35. Huarong, S.; Han, G.; Ling, P.; Zhu, X.; Wang, F.; Zhao, L.; Liu, F.; Liu, X.; Wang, G.; Ying, Y.; Zhang, T., Intra-articular injection of xanthan gum reduces pain and cartilage damage in a rat osteoarthritis model. Intra-articular injection of xanthan gum reduces pain and cartilage damage in a rat osteoarthritis model. *Carbohydrate Polymers* 2013, 92, 1850-1857. DOI: [10.1016/j.carbpol.2012.11.051](https://doi.org/10.1016/j.carbpol.2012.11.051).

36. Hu, L.; Yin, C.; Zhao, F.; Ali, A.; Ma, J.; Qian, A., Mesenchymal Stem Cells: Cell Fate Decision to Osteoblast or Adipocyte and Application in Osteoporosis Treatment. *International Journal of Molecular Sciences* 2018, 19 (2), 360.
37. Cho, S. W.; Sun, H. J.; Yang, J.-Y.; Jung, J. Y.; Choi, H. J.; An, J. H.; Kim, S. W.; Kim, S. Y.; Park, K.-J.; Shin, C. S., Human Adipose Tissue-Derived Stromal Cell Therapy Prevents Bone Loss in Ovariectomized Nude Mouse. *Tissue Engineering Part A* 2012, 18 (9-10), 1067-1078. DOI: 10.1089/ten.tea.2011.0355.
38. Bou-Francis, A.; Widmer Soyka, R. P.; Ferguson, S. J.; Hall, R. M.; Kapur, N., Novel methodology for assessing biomaterial–biofluid interaction in cancellous bone. *Journal of the Mechanical Behavior of Biomedical Materials* 2015, 46, 158-167. DOI: <https://doi.org/10.1016/j.jmbbm.2015.02.027>.
39. Baroud, G., Injection biomechanics of bone cements used in vertebroplasty. *Biomed Mater Eng* 2004, 14, 487-504.
40. Baroud, G.; Bohner, M., Biomechanical impact of vertebroplasty. *Joint Bone Spine* 2006, 73 (2), 144-150. DOI: <https://doi.org/10.1016/j.jbspin.2005.02.004>.
41. Bohner, M.; Gasser, B.; Baroud, G.; Heini, P., Theoretical and experimental model to describe the injection of a polymethylmethacrylate cement into a porous structure. *Biomaterials* 2003, 24 (16), 2721-2730. DOI: [https://doi.org/10.1016/S0142-9612\(03\)00086-3](https://doi.org/10.1016/S0142-9612(03)00086-3).
42. Murphy, W. L.; McDevitt, T. C.; Engler, A. J., Materials as stem cell regulators. *Nature Materials* 2014, 13, 547. DOI: 10.1038/nmat3937.
43. Bohner, M.; Baroud, G., Injectability of calcium phosphate pastes. *Biomaterials* 2005, 26 (13), 1553-1563. DOI: <https://doi.org/10.1016/j.biomaterials.2004.05.010>.

